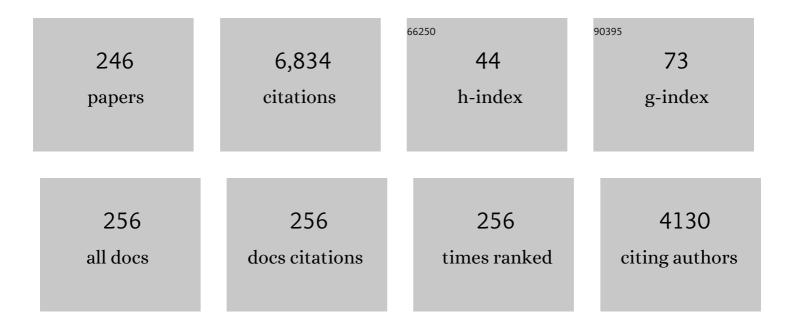
List of Publications by Year in descending order

Source: https://exaly.com/author-pdf/5788830/publications.pdf Version: 2024-02-01



#	Article	IF	CITATIONS
1	Improved Drainage Cannula Design to Reduce Thrombosis in Veno-Arterial Extracorporeal Membrane Oxygenation. ASAIO Journal, 2022, 68, 205-213.	0.9	12
2	Turbulent cylinder-stirred flow heat and momentum transfer research in batch operated single-phase square reactor. International Journal of Thermal Sciences, 2022, 172, 107325.	2.6	3
3	Influence of Eddy Viscosity on Linear Modeling of Self-Similar Coherent Structures in the Jet Far Field. , 2022, , .		5
4	Combining experimental and computational techniques to understand and improve dry powder inhalers. Expert Opinion on Drug Delivery, 2022, 19, 59-73.	2.4	8
5	Unraveling the Kinematics of Sperm Motion by Reconstructing the Flagellar Wave Motion in 3D. Small Methods, 2022, 6, e2101089.	4.6	10
6	Investigating Shear-Layer Instabilities in Supersonic Impinging Jets Using Dual-Time Particle Image Velocimetry. AIAA Journal, 2022, 60, 3749-3759.	1.5	3
7	In-vitro and particle image velocimetry studies of dry powder inhalers. International Journal of Pharmaceutics, 2021, 592, 119966.	2.6	18
8	The generation of screech tones by shock leakage. Journal of Fluid Mechanics, 2021, 908, .	1.4	26
9	Intermittent modal coupling in screeching underexpanded circular twin jets. Journal of Fluid Mechanics, 2021, 910, .	1.4	15
10	On the Use of Computational Fluid Dynamics (CFD) Modelling to Design Improved Dry Powder Inhalers. Pharmaceutical Research, 2021, 38, 277-288.	1.7	13
11	Simulation and characterization of the laminar separation bubble over a NACA-0012 airfoil as a function of angle of attack. Physical Review Fluids, 2021, 6, .	1.0	15
12	Flagellar energetics from high-resolution imaging of beating patterns in tethered mouse sperm. ELife, 2021, 10, .	2.8	19
13	Linear modelling of self-similar jet turbulence. Journal of Fluid Mechanics, 2021, 919, .	1.4	6
14	CRISPs Function to Boost Sperm Power Output and Motility. Frontiers in Cell and Developmental Biology, 2021, 9, 693258.	1.8	7
15	Distortion correction of two-component two-dimensional PIV using a large imaging sensor with application to measurements of a turbulent boundary layer flow at \$\$hbox {Re}_{au } = 2386\$\$. Experiments in Fluids, 2021, 62, 1.	1.1	1
16	Particle Image Velocimetry Measurements of a Dry Powder Inhaler Flow. International Symposium on Particle Image Velocimetry, 2021, 1, .	0.1	1
17	On assuring the accurate parallel alignment of a laser sheet for planar and stereoscopic particle image velocimetry. Experiments in Fluids, 2021, 62, 1.	1.1	0
18	Investigation of large scale motions in zero and adverse pressure gradient turbulent boundary layers using high-spatial-resolution particle image velocimetry. Experimental Thermal and Fluid Science, 2021, 129, 110469.	1.5	5

#	Article	IF	CITATIONS
19	Influence of nozzle external geometry on wavepackets in under-expanded supersonic impinging jets. Journal of Fluid Mechanics, 2021, 929, .	1.4	5
20	Analysis of a drag reduced flat plate turbulent boundary layer via uniform momentum zones. Aerospace Science and Technology, 2020, 96, 105552.	2.5	20
21	Near and far field laminar flow structures in an axisymmetric zero-net-mass-flux jet. Aerospace Science and Technology, 2020, 105, 105920.	2.5	6
22	Investigation of the Low-Frequency Oscillations in the Flowfield About an Airfoil. AIAA Journal, 2020, 58, 4271-4286.	1.5	9
23	Analysis of the spanwise extent and time persistence of uniform momentum zones in zero pressure gradient and adverse pressure gradient turbulent boundary layers. Journal of Physics: Conference Series, 2020, 1522, 012013.	0.3	2
24	Effect of limited near-wall inlet data on the direct numerical simulation of turbulent channel flow. Journal of Physics: Conference Series, 2020, 1522, 012019.	0.3	1
25	Characteristics of acoustic and hydrodynamic waves in under-expanded supersonic impinging jets. Journal of Fluid Mechanics, 2020, 905, .	1.4	13
26	Assessment of three-dimensional density measurements from tomographic background-oriented schlieren (BOS). Measurement Science and Technology, 2020, 31, 114002.	1.4	18
27	Characterisation of uniform momentum zones in adverse pressure gradient turbulent boundary layers. Experimental Thermal and Fluid Science, 2020, 115, 110080.	1.5	6
28	Measurement and analysis of the shear layer instabilities in supersonic impinging jets. , 2020, , .		2
29	Application of a POD-Galerkin based method to time resolved and time unresolved data for the determination of the Convective Velocity of Large-Scale Coherent Structures in High Speed Flows. International Journal of Heat and Fluid Flow, 2020, 85, 108647.	1.1	3
30	Analysis of the factors contributing to the skin friction coefficient in adverse pressure gradient turbulent boundary layers and their variation with the pressure gradient. International Journal of Heat and Fluid Flow, 2020, 82, 108531.	1.1	6
31	Receptivity characteristics of under-expanded supersonic impinging jets. Journal of Fluid Mechanics, 2020, 889, .	1.4	19
32	A novel 4D digital holographic PIV/PTV (4D-DHPIV/PTV) methodology using iterative predictive inverse reconstruction. Measurement Science and Technology, 2020, 31, 104002.	1.4	8
33	Volumetric measurements of a self-similar adverse pressure gradient turbulent boundary layer using single-camera light-field particle image velocimetry. Experiments in Fluids, 2019, 60, 1.	1.1	12
34	High-order accurate large-eddy simulations of compressible viscous flow in cylindrical coordinates. Computers and Fluids, 2019, 191, 104241.	1.3	13
35	High resolution volumetric dual-camera light-field PIV. Experiments in Fluids, 2019, 60, 1.	1.1	19
36	Nozzle external geometry as a boundary condition for the azimuthal mode selection in an impinging underexpanded jet. Journal of Fluid Mechanics, 2019, 862, 421-448.	1.4	37

#	Article	IF	CITATIONS
37	Effect of turbulence on drop breakup in counter air flow. International Journal of Multiphase Flow, 2019, 120, 103108.	1.6	9
38	The structure and dynamics of backflow in turbulent channels. Journal of Fluid Mechanics, 2019, 880,	1.4	23
39	Dynamic stall in vertical axis wind turbines: scaling and topological considerations. Journal of Fluid Mechanics, 2018, 841, 746-766.	1.4	63
40	Linearised dynamics and non-modal instability analysis of an impinging under-expanded supersonic jet. Journal of Physics: Conference Series, 2018, 1001, 012019.	0.3	6
41	A detailed comparison of single-camera light-field PIV and tomographic PIV. Experiments in Fluids, 2018, 59, 1.	1.1	40
42	The size dependant behaviour of particles driven by a travelling surface acoustic wave (TSAW). Lab on A Chip, 2018, 18, 3926-3938.	3.1	50
43	Characterisation of minimal-span plane Couette turbulence with pressure gradients. Journal of Physics: Conference Series, 2018, 1001, 012020.	0.3	0
44	Signatures of shear-layer unsteadiness in proper orthogonal decomposition. Experiments in Fluids, 2018, 59, 1.	1.1	19
45	Analysis of Coherent Structures in an Under-Expanded Supersonic Impinging Jet Using Spectral Proper Orthogonal Decomposition (SPOD). Aerospace, 2018, 5, 73.	1.1	25
46	Upstream-travelling acoustic jet modes as a closure mechanism for screech. Journal of Fluid Mechanics, 2018, 855, .	1.4	101
47	Coupling Modes of an Underexpanded Twin Axisymmetric Jet. AIAA Journal, 2018, 56, 3524-3535.	1.5	33
48	The influence of the cavity in the flow structures of a zero-net-mass-flux jet. , 2018, , .		0
49	Sound production by shock leakage in supersonic jet screech. , 2018, , .		9
50	An experimental investigation of coupled underexpanded supersonic twin-jets. Experiments in Fluids, 2018, 59, 1.	1.1	19
51	Reynolds stress structures in a self-similar adverse pressure gradient turbulent boundary layer at the verge of separation Journal of Physics: Conference Series, 2018, 1001, 012001.	0.3	2
52	Experimental evidence of near-wall reverse flow events in a zero pressure gradient turbulent boundary layer. Experimental Thermal and Fluid Science, 2018, 91, 320-328.	1.5	39
53	An explanation for the phase lag in supersonic jet impingement. Journal of Fluid Mechanics, 2017, 815, .	1.4	45
54	Novel Method for Investigating Broadband Velocity Fluctuations in Axisymmetric Screeching Jets. AIAA Journal, 2017, 55, 2321-2334.	1.5	19

#	Article	IF	CITATIONS
55	Stability and three-dimensional evolution of aÂtransitional dynamic stall vortex. Journal of Fluid Mechanics, 2017, 823, 166-197.	1.4	14
56	On the Effects of Nozzle Lip Thickness on the Azimuthal Mode Selection of a Supersonic Impinging Flow. , 2017, , .		5
57	On the behaviour of impinging zero-net-mass-flux jets. Journal of Fluid Mechanics, 2017, 810, 25-59.	1.4	55
58	Direct numerical simulation of a self-similar adverse pressure gradient turbulent boundary layer at the verge of separation. Journal of Fluid Mechanics, 2017, 829, 392-419.	1.4	58
59	Near-wall statistics of a turbulent pipe flow at shear Reynolds numbers up to 40Â000. Journal of Fluid Mechanics, 2017, 826, .	1.4	47
60	Higher order dynamic mode decomposition of noisy experimental data: The flow structure of a zero-net-mass-flux jet. Experimental Thermal and Fluid Science, 2017, 88, 336-353.	1.5	105
61	Light-field camera-based 3D volumetric particle image velocimetry with dense ray tracing reconstruction technique. Experiments in Fluids, 2017, 58, 1.	1.1	42
62	Extensive characterisation of a high Reynolds number decelerating boundary layer using advanced optical metrology. Journal of Turbulence, 2017, 18, 929-972.	0.5	32
63	Scale and Reynolds number dependence of stochastic subgrid energy transfer in turbulent channel flow. Computers and Fluids, 2017, 151, 132-143.	1.3	2
64	Towards the Direct Numerical Simulation of a Self-similar Adverse Pressure Gradient Turbulent Boundary Layer Flow. , 2017, , 61-75.		2
65	Particle Image Velocimetry Analysis of the Twin Supersonic Jet Structure and Standing-Wave. , 2017, , .		3
66	Local topology via the invariants of the velocity gradient tensor within vortex clusters and intense Reynolds stress structures in turbulent channel flow. Journal of Physics: Conference Series, 2016, 708, 012005.	0.3	4
67	Inception and evolution of coherent structures in under-expanded supersonic jets. Journal of Physics: Conference Series, 2016, 708, 012015.	0.3	5
68	Scaling and statistics of large-defect adverse pressure gradient turbulent boundary layers. International Journal of Heat and Fluid Flow, 2016, 59, 109-124.	1.1	36
69	Formation of Three-Dimensional Structures in the Hemisphere-Cylinder. AIAA Journal, 2016, 54, 3884-3894.	1.5	10
70	Experimental analysis of particle sizes for PIV measurements. Measurement Science and Technology, 2016, 27, 094009.	1.4	1
71	Direct numerical simulation of a self-similar adverse pressure gradient turbulent boundary layer. International Journal of Heat and Fluid Flow, 2016, 61, 129-136.	1.1	42
72	Impingement Tones and Associated Shock Instabilities in Supersonic Plug Nozzle Flows. AIAA Journal, 2016, 54, 2843-2851.	1.5	2

JULIO SORIA

#	Article	IF	CITATIONS
73	Supersonic Jet Impingement on a Cylindrical Surface. , 2016, , .		7
74	A Novel Method for Decoupling the Velocity Fluctuations in Screeching Axisymmetric Jets. , 2016, , .		1
75	Pre-detachment Acoustic Emission of a Bubble Emerging from an Orifice. Lecture Notes in Mechanical Engineering, 2016, , 119-123.	0.3	0
76	Evaluation of a film-based wall shear stress measurement technique in a turbulent channel flow. Experimental Thermal and Fluid Science, 2016, 70, 437-442.	1.5	6
77	On the identification of intense Reynolds stress structures in wall-bounded flows using information-limited two-dimensional planar data. European Journal of Mechanics, B/Fluids, 2016, 55, 279-285.	1.2	2
78	Insights into Spray Development from Metered-Dose Inhalers Through Quantitative X-ray Radiography. Pharmaceutical Research, 2016, 33, 1249-1258.	1.7	9
79	Efficiency of the lumped parameter concept and the role of liquid properties in modelling microdroplet evaporation. Fuel, 2016, 166, 86-95.	3.4	3
80	Boundary Condition Development for an Adverse Pressure Gradient Turbulent Boundary Layer at the Verge of Separation. , 2016, , 269-278.		1
81	Decomposition of Radiating and Non-Radiating Linear Fluctuating Components in Compressible Flows. , 2016, , 388-396.		0
82	Scale Dependent Stochastic Self-energy Model of the Energy Transfers in Turbulent Channel Flows. Springer Proceedings in Physics, 2016, , 139-143.	0.1	0
83	Stability Analysis of Time-averaged Jet Flows: Fundamentals and Application. Procedia IUTAM, 2015, 14, 141-146.	1.2	2
84	Staging Behaviour in Screeching Elliptical Jets. International Journal of Aeroacoustics, 2015, 14, 1005-1024.	0.8	21
85	Staging behaviour in screeching elliptical jets. International Journal of Aeroacoustics, 2015, 14, 1005-1024.	0.8	3
86	Shock structures and instabilities formed in an underexpanded jet impinging on to cylindrical sections. Shock Waves, 2015, 25, 611-622.	1.0	27
87	Multimodal Instability in the Weakly Underexpanded Elliptic Jet. AIAA Journal, 2015, 53, 2739-2749.	1.5	25
88	Investigation of Coherent Structures and Dynamics Using POD and DMD of a Separated Airfoil Subjected to ZNMF Jet Forcing. Fluid Mechanics and Its Applications, 2015, , 33-38.	0.1	1
89	An Experimental Investigation of Turbulent Convection Velocities in a Turbulent Boundary Layer. Flow, Turbulence and Combustion, 2015, 94, 79-95.	1.4	28
90	On the role of pressure in elasto-inertial turbulence. Journal of Turbulence, 2015, 16, 26-43.	0.5	30

#	Article	IF	CITATIONS
91	The growth of instabilities in annular liquid sheets. Experimental Thermal and Fluid Science, 2015, 68, 89-99.	1.5	15
92	Flow around a hemisphere-cylinder at high angle of attack and low Reynolds number. Part II: POD and DMD applied to reduced domains. Aerospace Science and Technology, 2015, 44, 88-100.	2.5	41
93	Proposed stochastic parameterisations of subgrid turbulence in large eddy simulations of turbulent channel flow. Journal of Turbulence, 2015, 16, 729-741.	0.5	6
94	Application of a single-board computer as a low-cost pulse generator. Measurement Science and Technology, 2015, 26, 095302.	1.4	19
95	Dynamic stall in vertical axis wind turbines: Comparing experiments and computations. Journal of Wind Engineering and Industrial Aerodynamics, 2015, 146, 163-171.	1.7	106
96	Measuring shear layer growth rates in aeroacoustically forced axisymmetric supersonic jets. , 2015, , .		7
97	Measurements of the flow due to a rapidly pitching plate using time resolved high resolution PIV. Aerospace Science and Technology, 2015, 44, 4-17.	2.5	9
98	Flow around a hemisphere-cylinder at high angle of attack and low Reynolds number. Part I: Experimental and numerical investigation. Aerospace Science and Technology, 2015, 44, 77-87.	2.5	38
99	Three-Dimensional Waves Inside an Open Cavity and Interactions with the Impinging Shear Layer. Fluid Mechanics and Its Applications, 2015, , 209-214.	0.1	0
100	Prologue to the International Conference on Massively Separated Flows and Their Control. Fluid Mechanics and Its Applications, 2015, , 1-3.	0.1	0
101	Numerical issues in Lagrangian tracking and topological evolution of fluid particles in wall-bounded turbulent flows. Journal of Physics: Conference Series, 2014, 506, 012003.	0.3	0
102	Instability Modes in Screeching Elliptical Jets. , 2014, , .		6
103	The underexpanded jet Mach disk and its associated shear layer. Physics of Fluids, 2014, 26, .	1.6	71
104	Coherent structure and sound production in the helical mode of a screeching axisymmetric jet. Journal of Fluid Mechanics, 2014, 748, 822-847.	1.4	109
105	Mean flow stability analysis of oscillating jet experiments. Journal of Fluid Mechanics, 2014, 757, 1-32.	1.4	41
106	On the modulating effect of three-dimensional instabilities in open cavity flows. Journal of Fluid Mechanics, 2014, 759, 546-578.	1.4	21
107	Large eddy simulation and Reynolds-averaged Navier-Stokes calculations of supersonic impinging jets at varying nozzle-to-wall distances and impinging angles. International Journal of Heat and Fluid Flow, 2014, 47, 31-41.	1.1	12
108	High spatial range velocity measurements in a high Reynolds number turbulent boundary layer. Physics of Fluids, 2014, 26, .	1.6	46

#	Article	IF	CITATIONS
109	Analysis of a Turbulent Boundary Layer Subjected to a Strong Adverse Pressure Gradient. Journal of Physics: Conference Series, 2014, 506, 012007.	0.3	14
110	On the appropriate filtering of PIV measurements of turbulent shear flows. Experiments in Fluids, 2014, 55, 1.	1.1	36
111	Stochastic self-energy subgrid model for the large eddy simulation of turbulent channel flows. Journal of Physics: Conference Series, 2014, 506, 012001.	0.3	3
112	Ultra-high-speed 3D astigmatic particle tracking velocimetry: application to particle-laden supersonic impinging jets. Experiments in Fluids, 2014, 55, 1.	1.1	16
113	A Novel High-Speed Imaging Technique to Predict the Macroscopic Spray Characteristics of Solution Based Pressurised Metered Dose Inhalers. Pharmaceutical Research, 2014, 31, 2963-2974.	1.7	14
114	Time-resolved stereo PIV measurements in the far-field of a turbulent zero-net-mass-flux jet. Experimental Thermal and Fluid Science, 2014, 57, 111-120.	1.5	4
115	Skin-friction critical points in wall-bounded flows. Journal of Physics: Conference Series, 2014, 506, 012009.	0.3	13
116	Three-dimensional instabilities over a rectangular open cavity: from linear stability analysis to experimentation. Journal of Fluid Mechanics, 2014, 748, 189-220.	1.4	53
117	Three-dimensional instabilities over a rectangular open cavity: from linear stability analysis to experimentation – ERRATUM. Journal of Fluid Mechanics, 2014, 751, 747-748.	1.4	3
118	Analysis of the anisotropy of group velocity error due to spatial finite difference schemes from the solution of the 2D linear Euler equations. International Journal for Numerical Methods in Fluids, 2013, 71, 805-829.	0.9	2
119	Near-field structure of underexpanded elliptic jets. Experiments in Fluids, 2013, 54, 1.	1.1	59
120	Time-resolved PIV measurements of the flow field in a stenosed, compliant arterial model. Experiments in Fluids, 2013, 54, 1.	1.1	30
121	Evolution of the turbulent/non-turbulent interface of an axisymmetric turbulent jet. Experiments in Fluids, 2013, 54, 1.	1.1	29
122	Influence of ZNMF jet flow control on the spatio-temporal flow structure over a NACA-0015 airfoil. Experiments in Fluids, 2013, 54, 1.	1.1	50
123	Microdroplet evaporation under increasing temperature conditions: Experiments and modelling. Fuel, 2013, 105, 247-257.	3.4	21
124	Investigation of the Flow Structures in Supersonic Free and Impinging Jet Flows. Journal of Fluids Engineering, Transactions of the ASME, 2013, 135, .	0.8	34
125	Computationally efficient storage of 3D particle intensity and position data for use in 3D PIV and 3D PTV. Measurement Science and Technology, 2013, 24, 115303.	1.4	3
126	On the mechanism of elasto-inertial turbulence. Physics of Fluids, 2013, 25, 110817.	1.6	121

#	Article	IF	CITATIONS
127	Ultra-high-speed tomographic digital holographic velocimetry in supersonic particle-laden jet flows. Measurement Science and Technology, 2013, 24, 024005.	1.4	51
128	Structural analysis on a hemisphere-cylinder at moderate Reynolds number and high angle of attack. , 2013, , .		1
129	Measurements of the Three-Dimensional Topological Evolution of a Dynamic Stall Event Using Wavelet Methods. , 2013, , .		0
130	An improved interpolation scheme for finite volume simulations on unstructured meshes. Mathematics of Computation, 2012, 82, 803-830.	1.1	0
131	On measuring the joint probability density function of three-dimensional velocity components in turbulent flows. Measurement Science and Technology, 2012, 23, 065301.	1.4	9
132	Lagrangian evolution of the invariants of the velocity gradient tensor in a turbulent boundary layer. Physics of Fluids, 2012, 24, .	1.6	22
133	Experimental investigation of nonlinear instabilities in annular liquid sheets. Journal of Fluid Mechanics, 2012, 691, 594-604.	1.4	62
134	Ultra-High-Speed Digital In-Line Holography System Applied to Particle-Laden Supersonic Underexpanded Jet Flows. , 2012, , .		3
135	Time-resolved Particle Image Velocimetry and Structural Analysis on An Hemisphere-Cylinder at Low Reynolds Numbers and Large Angle of Incidence. , 2012, , .		2
136	The visualization of the acoustic feedback loop in impinging underexpanded supersonic jet flows using ultra-high frame rate schlieren. Journal of Visualization, 2012, 15, 333-341.	1.1	71
137	Pulsed, high-power LED illumination for tomographic particle image velocimetry. Experiments in Fluids, 2012, 53, 1545-1560.	1.1	37
138	An assessment of high-power light-emitting diodes for high frame rate schlieren imaging. Experiments in Fluids, 2012, 53, 413-421.	1.1	119
139	A new perspective on spectral analysis of numerical schemes. International Journal for Numerical Methods in Fluids, 2012, 68, 467-482.	0.9	3
140	A Numerical Investigation of the Cold Spray Process Using Underexpanded and Overexpanded Jets. Journal of Thermal Spray Technology, 2012, 21, 108-120.	1.6	34
141	Stereoscopic and tomographic PIV of a pitching plate. Experiments in Fluids, 2012, 52, 299-314.	1.1	27
142	An error analysis of the dynamic mode decomposition. Experiments in Fluids, 2012, 52, 529-542.	1.1	131
143	A Comparison of Subpixel Edge Detection and Correlation Algorithms for the Measurement of Sprays. International Journal of Spray and Combustion Dynamics, 2011, 3, 93-109.	0.4	13
144	Measurements of Near Wall Velocity and Wall Stress in a Wall-Bounded Turbulent Flow Using Digital Holographic Microscopic PIV and Shear Stress Sensitive Film. ERCOFTAC Series, 2011, , 385-392.	0.1	0

#	Article	IF	CITATIONS
145	Three-Dimensional Substructure in a Leading Edge Vortex. , 2011, , .		0
146	Study of Vortical Structures in Turbulent Near-Wall Flows. ERCOFTAC Series, 2011, , 121-131.	0.1	0
147	Topology and dynamics of flow structures in wall-bounded turbulent flows. Journal of Physics: Conference Series, 2011, 318, 062018.	0.3	3
148	On the coherent structures and stability properties of a leading-edge separated aerofoil with turbulent recirculation. Journal of Fluid Mechanics, 2011, 683, 395-416.	1.4	55
149	Measuring evaporation of micro-fuel droplets using magnified DIH and DPIV. Experiments in Fluids, 2011, 50, 949-959.	1.1	18
150	The accuracy of tomographic particle image velocimetry for measurements of a turbulent boundary layer. Experiments in Fluids, 2011, 50, 1031-1056.	1,1	97
151	A film-based wall shear stress sensor for wall-bounded turbulent flows. Experiments in Fluids, 2011, 51, 137-147.	1.1	13
152	Tomographic particle image velocimetry investigation of the flow in a modeled human carotid artery bifurcation. Experiments in Fluids, 2011, 50, 1131-1151.	1.1	51
153	Editorial: PIV'09 special issue. Experiments in Fluids, 2011, 50, 775-775.	1.1	1
154	A correlation image velocimetry-based study of high-pressure fuel spray tip evolution. Experiments in Fluids, 2011, 51, 667-678.	1.1	20
155	Particle relaxation and its influence on the particle image velocimetry cross-correlation function. Experiments in Fluids, 2011, 51, 933-947.	1.1	40
156	Investigation of wall-bounded turbulent flow using Dynamic mode decomposition. Journal of Physics: Conference Series, 2011, 318, 042040.	0.3	9
157	Tomographic Particle Image Velocimetry Measurements of a High Reynolds Number Turbulent Boundary Layer. ERCOFTAC Series, 2011, , 113-120.	0.1	1
158	Axial plus tangential entry swirling jet. Experiments in Fluids, 2010, 48, 309-325.	1.1	61
159	A cross-correlation velocimetry technique for breakup of an annular liquid sheet. Experiments in Fluids, 2010, 49, 435-445.	1.1	45
160	The effect of internal diffusion on an evaporating bio-oil droplet – The chemistry free case. Biomass and Bioenergy, 2010, 34, 1134-1140.	2.9	15
161	Development of a nonlinear eddy-viscosity closure for the triple-decomposition stability analysis of a turbulent channel. Journal of Fluid Mechanics, 2010, 664, 74-107.	1.4	26
162	Multi-Component - Multi-Dimensional PIV Measurements for a Flat-Plate Pitching Motion. , 2010, , .		1

#	Article	IF	CITATIONS
163	The organization of near-wall turbulence: a comparison between boundary layer SPIV data and channel flow DNS data. Journal of Turbulence, 2010, 11, N47.	0.5	24
164	Effect of nozzle transients and compressibility on the penetration of fuel sprays. Applied Physics Letters, 2009, 95, .	1.5	25
165	An efficient simultaneous reconstruction technique for tomographic particle image velocimetry. Experiments in Fluids, 2009, 47, 553-568.	1.1	215
166	Time resolved measurements of the initial stages of fuel spray penetration. Fuel, 2009, 88, 2225-2237.	3.4	87
167	A singularity-avoiding moving least squares scheme for two-dimensional unstructured meshes. Journal of Computational Physics, 2009, 228, 5592-5619.	1.9	10
168	BiGlobal stability analysis in curvilinear coordinates of massively separated lifting bodies. Journal of Computational Physics, 2009, 228, 7181-7196.	1.9	38
169	Multi-Component, Multi-Dimensional PIV Measurements of Low Reynolds Number Flow Around Flat Plate Undergoing Pitch-Ramp Motion. , 2009, , .		2
170	DHMPIV and Tomo-PIV measurements of three-dimensional structures in a turbulent boundary layer. Springer Proceedings in Physics, 2009, , 613-616.	0.1	1
171	In-Vitro Investigation of three-dimensional Carotid Artery Haemodynamics by Tomographic Particle Image Velocimetry. IFMBE Proceedings, 2009, , 1665-1668.	0.2	0
172	Fluid mechanics of flapping wings. Experimental Thermal and Fluid Science, 2008, 32, 1578-1589.	1.5	46
173	High-speed visualisation of primary break-up of an annular liquid sheet. Experiments in Fluids, 2008, 44, 451-459.	1.1	52
174	Stereoscopic PIV measurements of a turbulent boundary layer with a large spatial dynamic range. Experiments in Fluids, 2008, 45, 745-763.	1.1	44
175	Use of zero-net-mass-flow for separation control in diffusing S-duct. Experimental Thermal and Fluid Science, 2008, 33, 169-172.	1.5	20
176	BiGlobal Instability Analysis of Turbulent Flow Over an Airfoil at an Angle of Attack. , 2008, , .		4
177	Measuring dynamic phenomena at the sub-micron scale. , 2008, , .		2
178	Separation control on a NACA 0015 airfoil using a 2D micro ZNMF jet. Aircraft Engineering and Aerospace Technology, 2008, 80, 175-180.	0.8	28
179	Towards 3C-3D digital holographic fluid velocity vector field measurement—tomographic digital holographic PIV (Tomo-HPIV). Measurement Science and Technology, 2008, 19, 074002.	1.4	75
180	Characterisation of the mean flow of a micro-injector induced swirling jet. Australian Journal of Mechanical Engineering, 2008, 5, 51-58.	1.5	0

#	Article	IF	CITATIONS
181	Direct Numerical Simulation of passive scalar mixing in axisymmetric swirling jets. Australian Journal of Mechanical Engineering, 2008, 5, 71-80.	1.5	0
182	High-speed optical measurements of an underexpanded supersonic jet impinging on an inclined plate. Proceedings of SPIE, 2008, , .	0.8	16
183	Thrust Measurements from a Finite-Span Flapping Wing. AIAA Journal, 2007, 45, 58-70.	1.5	18
184	Accelerated flow past a symmetric aerofoil: experiments and computations. Journal of Fluid Mechanics, 2007, 591, 255-288.	1.4	17
185	Morphology of the forced oscillatory flow past a finite-span wing at low Reynolds number. Journal of Fluid Mechanics, 2007, 571, 327-357.	1.4	28
186	Direct numerical simulation of passive scalars mixing in an axisymmetric swirl induced vortex breakdown flow. Australian Journal of Mechanical Engineering, 2007, 4, 15-28.	1.5	1
187	Digital holography for micro-droplet diagnostics. Experiments in Fluids, 2007, 43, 185-195.	1.1	37
188	High Spatial Resolution MCCDPIV in a Zero Pressure Gradient Turbulent Boundary Layer. , 2007, , 773-773.		0
189	Characteristics of the Vortex Street Behind a Finite Aspect-Ratio Flapping Wing. , 2006, , .		1
190	Experimental Study of the Near Jet Region of a Pulsed Free Jet Using MCCDPIV. , 2006, , .		0
191	Laser-based planar imaging of nano-particle fluidization: Part l—determination of aggregate size and shape. Chemical Engineering Science, 2006, 61, 5476-5486.	1.9	61
192	Combustion properties of slow pyrolysis bio-oil produced from indigenous Australian species. Renewable Energy, 2006, 31, 2108-2121.	4.3	59
193	Laser-based planar imaging of nano-particle fluidization: Part II—mechanistic analysis of nanoparticle aggregation. Chemical Engineering Science, 2006, 61, 8040-8049.	1.9	33
194	Particle Image Velocimetry - Application to Turbulence Studies. World Scientific Lecture Notes in Complex Systems, 2006, , 309-347.	0.1	7
195	PARTICLE IMAGE VELOCIMETRY MEASUREMENTS AND CFD ANALYSIS OF AN UNDEREXPANDED SUPERSONIC JET. , 2006, , .		3
196	Flow Visualisations and PIV Measurements of ZNMF Jet Control of Separated Flow Over NACA0015 Airfoil. , 2006, , .		0
197	The relationship between the topological structures in turbulent flow and the distribution of a passive scalar with an imposed mean gradient. Fluid Dynamics Research, 2005, 36, 107-120.	0.6	10
198	A comparison between snapshot POD analysis of PIV velocity and vorticity data. Experiments in Fluids, 2005, 38, 146-160.	1.1	145

#	Article	IF	CITATIONS
199	Using stereo multigrid DPIV (SMDPIV) measurements to investigate the vortical skeleton behind a finite-span flapping wing. Experiments in Fluids, 2005, 39, 281-298.	1.1	46
200	Visualization of Flow Development in Hybrid Rocket Motors with High Regression Rates. Journal of Propulsion and Power, 2005, 21, 613-619.	1.3	3
201	Investigation of the mean passive scalar field in zero-net-mass-flux jets in cross-flow using planar-laser-induced fluorescence. Physics of Fluids, 2004, 16, 794-808.	1.6	27
202	The stability of low Reynolds number round jets. Experiments in Fluids, 2004, 36, 473-483.	1.1	55
203	Near-field pairing of leading-edge vortices in elliptic jets in cross flow. European Journal of Mechanics, B/Fluids, 2004, 23, 551-569.	1.2	7
204	The interaction of the piston vortex with a piston-generated vortex ring. Journal of Fluid Mechanics, 2004, 499, 327-343.	1.4	40
205	Multigrid CCDPIV measurements of accelerated flow past an airfoil at an angle of attack of 30°. Experimental Thermal and Fluid Science, 2003, 27, 667-676.	1.5	21
206	Flow structures behind a heaving and pitching finite-span wing. Journal of Fluid Mechanics, 2003, 490, 129-138.	1.4	177
207	Flow visualization of the effect of pitch amplitude changes on the vortical signatures behind a three-dimensional flapping airfoil. , 2003, , .		5
208	The evolution of round zero-net-mass-flux jets. Journal of Fluid Mechanics, 2002, 472, 167-200.	1.4	277
209	PIV measurements of a zero-net-mass-flux jet in cross flow. Experiments in Fluids, 2002, 33, 863-872.	1.1	48
210	Particle image velocimetry measurements of a backward-facing step flow. Experiments in Fluids, 2002, 33, 838-853.	1.1	134
211	5. The structure of a separated shear layer from a blunt leading edge under forcing. Journal of Visualization, 2001, 4, 119-119.	1.1	0
212	Measurements of a wall-bounded, turbulent, separated flow using HPIV. Journal of Turbulence, 2001, 2, N4.	0.5	17
213	Direct numerical simulations of vortex breakdown in swirling jets. Journal of Turbulence, 2001, 2, N5.	0.5	14
214	High resolution multigrid cross-correlation digital PIV measurements of a turbulent starting jet using half frame image shift film recording. Optics and Laser Technology, 1999, 31, 3-12.	2.2	31
215	Use of holography in particle image velocimetry measurements of a swirling flow. Experiments in Fluids, 1999, 27, 251-261.	1.1	24
216	A study of the evolution and characteristics of the invariants of the velocity-gradient tensor in isotropic turbulence. Journal of Fluid Mechanics, 1999, 381, 141-174.	1.4	202

#	Article	IF	CITATIONS
217	Accuracy of out-of-plane vorticity measurements derived from in-plane velocity field data. Experiments in Fluids, 1998, 25, 409-430.	1.1	113
218	Dynamics of the velocity gradient tensor invariants in isotropic turbulence. Physics of Fluids, 1998, 10, 2336-2346.	1.6	92
219	Turbulence structures of wall-bounded shear flows found using DNS data. Journal of Fluid Mechanics, 1998, 357, 225-247.	1.4	166
220	<title>High-resolution cross-correlation PIV on photographic film</title> ., 1998,,.		0
221	<title>Effect of anomalous particle light scattering on PIV image quality</title> . , 1998, , .		Ο
222	Vortex Ring Formation at an Orifice. Fluid Mechanics and Its Applications, 1998, , 15-18.	0.1	0
223	Flow Field Measurements of Separated and Reattached Flows. Fluid Mechanics and Its Applications, 1998, , 11-14.	0.1	Ο
224	The inverse diffusion time scale of velocity gradients in homogeneous isotropic turbulence. Physics of Fluids, 1997, 9, 814-816.	1.6	14
225	Volume integrals of theQA-RAinvariants of the velocity gradient tensor in incompressible flows. Fluid Dynamics Research, 1997, 19, 219-233.	0.6	11
226	Investigating flow topologies in boundary layer transition using direct numerical simulation. Flow, Turbulence and Combustion, 1996, 57, 367-382.	0.2	1
227	An investigation of the near wake of a circular cylinder using a video-based digital cross-correlation particle image velocimetry technique. Experimental Thermal and Fluid Science, 1996, 12, 221-233.	1.5	227
228	Shear layer vortices and longitudinal vortices in the near wake of a circular cylinder. Experimental Thermal and Fluid Science, 1996, 12, 169-174.	1.5	36
229	Behavior of an elastic fluid in cylindrical swirling flow. Experimental Thermal and Fluid Science, 1996, 12, 250-255.	1.5	18
230	Investigating Flow Topologies in Boundary Layer Transition by Numerical Simulation. Fluid Mechanics and Its Applications, 1996, , 59-60.	0.1	0
231	Reynolds Number Dependance of the Vorticity Alignment with the Three Principal Rates of Strain. Fluid Mechanics and Its Applications, 1996, , 255-258.	0.1	Ο
232	Laminar boundary layer receptivity to transverse structural vibration. Journal of Sound and Vibration, 1995, 186, 463-493.	2.1	1
233	Examination of the flow around a hot-wire probe using particle image velocimetry. Experiments in Fluids, 1995, 19, 379-382.	1.1	3
234	The Spatial Structure of Intense Foci in a Time-Developing Three-Dimensional Plane Wake. Fluid Mechanics and Its Applications, 1995, , 491-495.	0.1	0

#	Article	IF	CITATIONS
235	Topological visualisation of focal structures in free shear flows. Flow, Turbulence and Combustion, 1994, 53, 375-386.	0.2	20
236	An Experimental Investigation of Streamwise Vortices in the Wake of a Bluff Body. Journal of Fluids and Structures, 1994, 8, 621-625.	1.5	6
237	An experimental investigation of streamwise vortices in the wake of a bluff body. Journal of Fluids and Structures, 1994, 8, 621-635.	1.5	53
238	A study of the fineâ€scale motions of incompressible timeâ€developing mixing layers. Physics of Fluids, 1994, 6, 871-884.	1.6	190
239	Experimental investigation of vortex shedding from a plate: effect of external velocity perturbation. Journal of Wind Engineering and Industrial Aerodynamics, 1993, 49, 401-410.	1.7	3
240	Spatial evolution of the separated shear layer from a square leading-edge flat plate. Journal of Wind Engineering and Industrial Aerodynamics, 1993, 49, 237-246.	1.7	4
241	Identification and Classification of Topological Structures in Free Shear Flows. Fluid Mechanics and Its Applications, 1993, , 379-390.	0.1	14
242	The effect of transverse plate vibration on the mean laminar convective boundary layer heat transfer rate. Experimental Thermal and Fluid Science, 1991, 4, 226-238.	1.5	5
243	A simple-to-fabricate composite convective heat-transfer test surface. Applied Energy, 1990, 35, 109-123.	5.1	1
244	A study of unsteady laminar boundary layer flow on a flat plate using a smoke-wire/silhoutte flow visualization technique. Experimental Thermal and Fluid Science, 1990, 3, 291-304.	1.5	5
245	A study of the three-term hot-wire system equation and analog linearization based on it. Experimental Thermal and Fluid Science, 1990, 3, 346-353.	1.5	3
246	Estimation of Turbulent Dissipation Rate Using 2D Data in Channel Flows. , 0, , .		1